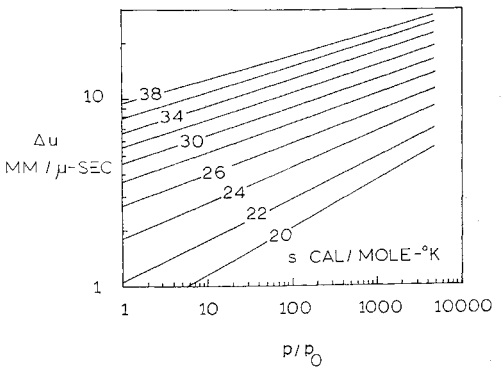

Fig. 3 Velocity increment resulting from a one-dimensional unsteady expansion in hydrogen.

known initial driver pressure and temperature, the corresponding entropy can be found from Fig. 2. Then from Fig. 3, the velocity increment resulting from the unsteady expansion is

$$u_f - u_i = \Delta u(p_i) - \Delta u(p_f) \quad (4)$$

Figure 4 reveals a significant difference between the performance of real and ideal hydrogen driving real air. For example, generation of a shock Mach number of 24 into real air at 300°K and 10^{-4} atm requires a pressure ratio p_4/p_1 about $2\frac{1}{2}$ times that of the ideal driver gas analysis.

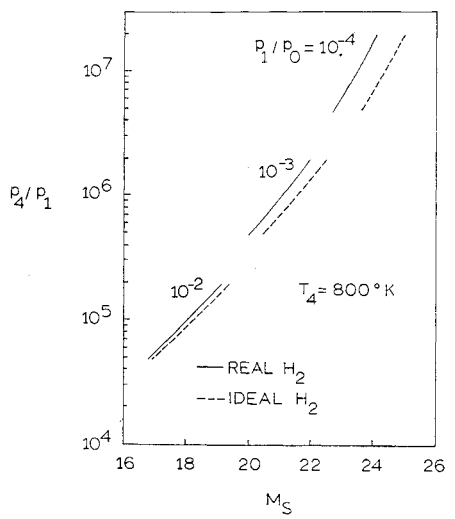

Fig. 4 Comparison of shock tube performance for real and ideal hydrogen driving real air.

References

[1] Smith, C. E., Hajjar, D. G., and Reinecke, W. G., "A Study of Large, High-Performance Shock Tunnel Drivers," TR AFAPL-TR-67-73, July 1967, Air Force Aero Propulsion Lab., Wright-Patterson Air Force Base, Ohio.

[2] Bird, K. D., Martin, J. F., and Bell, T. J., "Recent Developments in the Use of the Hypersonic Shock Tunnel as a Research and Development Facility," *Proceedings of the Third Hypervelocity Techniques Symposium*, Denver, Colorado, March 1964, pp. 7–50.

[3] Eschenroeder, A. Q., Daiber, J. W., Golian, T. C., and Hertzberg, A., "Shock Tunnel Studies of High-Enthalpy Ionized Airflows," CAL Report AF 1500-A-1, July 1962, Cornell Aeronautical Lab., Buffalo, N.Y.

[4] Bixler, D. N., Piacesi, R., and Seigel, A. E., "Calculated Thermodynamic Properties of Real Hydrogen Up to 30,000 Atmospheres and 3500°K," NOLTR 65-209, Ballistics Research Report 153, Dec. 1965, U.S. Naval Ordnance Lab., White Oak, Md.

[5] Huber, P. W., "Note on Hydrogen as a Rea Gas Driver for Shock Tubes," *Journal of the Aeronautical Sciences*, Vol. 25, No. 4, April, 1958, p. 269.

[6] Woolley, H. W., Scott, R. B., and Brickwedde, F. G., "Compilation of Thermal Properties of Hydrogen in its Various Isotopic and Ortho-Para Modifications," NBS Research Paper RP 1932, Vol. 41, Nov. 1948, National Bureau of Standards, Washington, D.C.

[7] Grose, W. L. and Trimpi, R. L., "Charts for the Analysis of Isentropic One-Dimensional Unsteady Expansions in Equilibrium Air with Particular Reference to Shock-Initiated Flows," TR R-167, 1963, NASA.

Downstream Pressure Distributions for Two-Dimensional Jet Interactions

M. J. Werle,* D. G. Shaffer,† and R. T. Driftmyer†
U.S. Naval Ordnance Laboratory, Silver Spring, Md.

Nomenclature

b^* = slot width, in.
b_e^* = $C_d b^*$, effective slot width, in.
C_d = jet nozzle discharge coefficient
F_{id} = downstream induced force
h_s = jet-shock height, in.
P = pressure, lbf/in.²
x = distance from jet slot, in.

Subscripts

j = jet conditions
o = stagnation conditions
peak = downstream peak conditions
s = separation conditions
∞ = freestream conditions

Introduction

THE general problem considered here is the use of reaction jets to generate control forces in a supersonic environment. A limited-scope, two-dimensional, experimental study has recently been completed at the Naval Ordnance Laboratory. This study is related to the definition of the controlling parameters for the surface pressure distributions aft of a secondary jet blowing normal to the supersonic mainstream. Only the case for turbulent separation forward of the jet was considered. Numerous authors have hinted that the forces produced downstream of the jet may well be beneficial for control purposes.[1,2,3] The only attempt to model this region was by Barnes et al.[1] using a limited amount of experimental data. The NOL study, with additional experimental data, found that the over-all behavior of the pressure distribution was different from that implied by the earlier study.

Equipment and Procedure

The present tests, with adiabatic wall conditions, were run with a freestream Mach number, $M_\infty = 4$, at two freestream Reynolds numbers, per foot, of 6×10^6 and 18×10^6. Shadowgraph pictures were taken of all test runs.[4] The test model was a flat plate 15.5 in. long and 10 in. wide fitted with a half-cylinder boundary-layer trip 0.025 in. high, located 0.75 in. from the leading edge. Surface flow studies using azobenzene, and complementary shadowgraph studies indicated that boundary-layer transition occurred 1.25 in.

Received December 15, 1969; revision received February 27, 1970. The research was sponsored by the Naval Air Systems Command (Air 320).

* Research Aerospace Engineer, Applied Aerodynamics Division and Assistant Professor, Engineering Mechanics Department, Virginia Polytechnic Institute.

† Aerospace Engineer, Applied Aerodynamics Division.

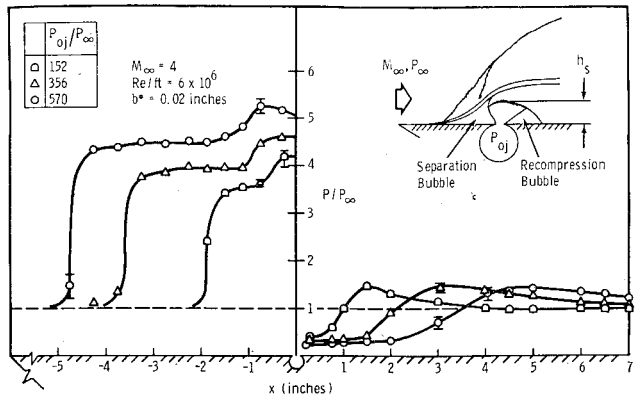

Fig. 1 Typical plate pressure distributions.

and 0.25 in. downstream of the trip for the low and high Reynolds numbers, respectively. Glass-ported side plates, mounted on the flat-plate surface, defined a 6-in.-wide flow channel, the surface of which was instrumented with 78 static-pressure taps. A removable 6-in. span jet-slot nozzle block was flush-mounted in the plate 7.25 in. from the leading edge. The sonic slots tested had nominal widths of $b^* = 0.005$, 0.020, and 0.030 in. Jet-gas mass-flow rates were monitored during all testing. It was found that the slots opened when pressurized. For this reason, an effective jet-slot width was defined as $b_e^* = C_d b^*$, where C_d is the mass-flow rate discharge coefficient of the jet slot. This was used in all subsequent calculations.

In all cases, the secondary-jet supply gas used was air at a total temperature of approximately 530°R. The jet total pressure, P_{oj}, was varied stepwise from zero up to that value for which the upstream separation line approached the boundary-layer trip, the maximum value being approximately 1200 psia for the 0.005-in. jet slot.

Results and Discussion

Figure 1 shows a typical set of plate pressure distributions fore and aft of a 0.020-in. jet slot at a Reynolds number, per foot, of 6×10^6. These data were measured over the center 2.75 in. of the plate surface. They are a valid representation of the two-dimensional problem since the data show little or no transverse gradients. Further, note in Fig. 1 that the upstream separation bubble increases with the jet strength, P_{oj}/P_∞, and that a similar growth is noted in both the downstream recompression bubble and the distance to the downstream peak pressure. There is strong evidence that the downstream peak pressure was independent of the jet strength, a result originally hinted at by Volz and Werle.[5] In addition, a universal pressure distribution was obtained by nondimensionalizing the downstream distributions by using the measured jet-shock height, h_s, as the characteristic length. This correlation is shown in Fig. 2 where the faired curve shown represents the average of all data taken for a given Reynolds number per foot. Outside of some scatter near the peak pressure, variations in the jet strength are completely accounted for in this correlation. The tendency towards a slight change in the downstream peak pressure with Reynolds number is not definitive enough to warrant a positive statement in this regard. However, the undisturbed upstream plate surface pressure was slightly greater than the freestream static pressure, P_∞, for both Reynolds numbers (see Fig. 1) and that it increased approximately 5% as the Reynolds number was decreased (apparently due to a boundary-layer trip interaction). This is roughly the same amount and in the same direction as the peak pressure changes observed in Fig. 2, the implication being that this change in peak pressure is due solely to a change in the P_∞ used to nondimensionalize the downstream pressures. Hence, it appears that the downstream distribution is solely a function of h_s, the Mach number being held constant. The pressure rise starts at $x/h_s \approx 2$ with $P/P_\infty \approx 0.4$, thereafter rising sharply to a peak at $x/h_s \approx 4.1$ with $P/P_\infty \approx 1.5$, followed by a decay back to the freestream pressure at $x/h_s \approx 12$. The net downstream side force is quite small where

$$\frac{F_{id}}{P_\infty h_s} = \int_0^\infty \left(\frac{P}{P_\infty} - 1\right) d\left(\frac{x}{h_s}\right) = 0.305 \qquad (1)$$

represents only about 2% of the force generated ahead of the jet, but within the accuracy of the measurements, $F_{id}/P_\infty h_s$ has to be taken as zero.

The pressure distribution downstream of a secondary jet has also been considered experimentally by Volz and Werle,[5] Spaid and Zukoski,[3] Cooper,[6] Kaufman,[2] and Barnes et al.[1] In Ref. 5, Volz and Werle used a scheme based on x_s, the forward separation distance, instead of h_s‡ and were able to correlate $M_\infty = 5$ downstream pressure distributions almost as well as those shown in Fig. 2. In that work they found the peak pressure to be about $P_{peak} = 2\,P_\infty$ and its position to be $x_{peak} = 0.5\,x_s$. In the present work at $M_\infty = 4$, x_s was found to be roughly linear with h_s, being given by

$$x_s = 5\,h_s \qquad (2)$$

so that the x_{peak} was at 0.8 x_s. Thus, there appears to be a

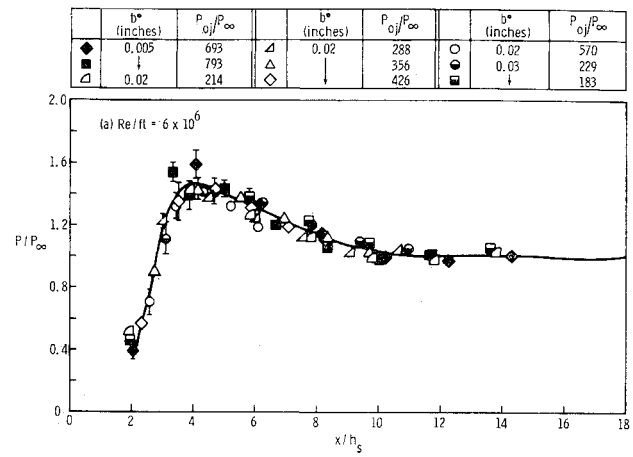

a) Low Reynolds number.

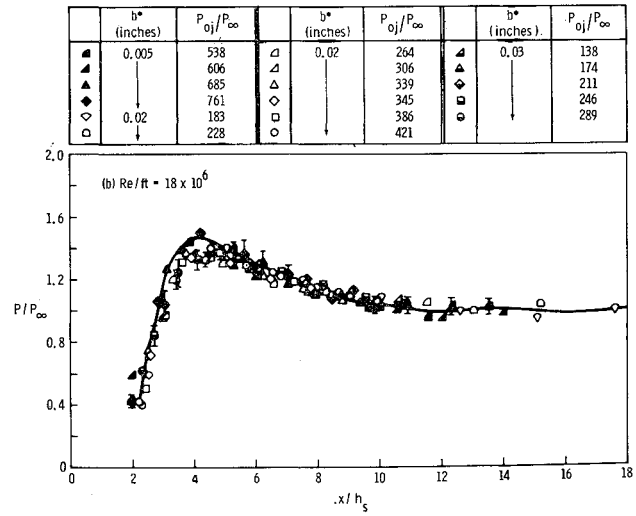

b) High Reynolds number.

Fig. 2 Downstream pressure distribution correlation.

‡ Volz and Werle were forced to use x_s because no shadowgraph data were available. The shock height, h_s, seems the more fundamental length for the downstream interaction region.

dependence of the peak pressure and its position on the free-stream Mach number. Further evidence to this effect was given by Spaid and Zukoski[3] who found experimentally that at $M_\infty = 2.61$, $P_{peak} = P_\infty$, while at $M_\infty = 3.5$, $P_{peak} = 1.1\ P_\infty$ and $x_{peak} \approx x_s$. Cooper[6] verified experimentally that at $M_\infty \approx 2.5$, $P_{peak} \approx P_\infty$. The very limited turbulent data presented by Barnes et al.[1] was interpreted by those authors as showing a dependence of P_{peak} on the jet-gas mass-flow rate with the maximum P_{peak} observed being approximately $4\ P_\infty$ at $M_\infty = 8$. Careful review of this data, though, (see Fig. 50 of Ref. 1) indicated that it would not be unreasonable to take a $P_{peak} = 4\ P_\infty$ at $x = 0.5\ x_s$ to $0.6\ x_s$ for the three jet-gas flow rates reported therein. Therefore, in contrast to the model proposed in Ref. 1, it appears that the downstream pressure distribution is characterized by a peak pressure which is completely independent of the jet-gas mass-flow rate. The level of this peak pressure is apparently only a function of freestream Mach number. No evidence was found in this test series to support Kaufman's suggestion[2] that P_{peak} depends linearly on $\bar{\chi} = 1 + M_\infty{}^3/(Re)^{1/2}$.

References

[1] Barnes, J. W., Davis, J. G., and Tang, H. H., "Control Effectiveness of Transverse Jets Interaction with a High-Speed Free Stream," AF-FDL-TR-67-90, Vol. 1, Sept. 1967, Wright-Patterson Air Force Base, Dayton, Ohio.

[2] Kaufman, L. G. (II) and Koch, F. (II), "High Speed Flow Past Transverse Jets," Rept. RE-348, Oct. 1968, Grumman Aircraft Engineering Corporation, Bethpage, N. Y.

[3] Spaid, F. W. and Zukoski, E. E., "A Study of the Interaction of Gaseous Jets from Transverse Slots with Supersonic External Flows," *AIAA Journal*, Vol. 6, No. 2, Feb. 1968, pp. 205–212.

[4] "Aero and Hydro Ballistics Research Facilities," NOLR 1264, July 1967, U. S. Naval Ordnance Laboratory, Silver Spring, Md.

[5] Volz, W. C. and Werle, M. J., "Jet Interaction Studies," Paper 40, *Proceedings of the 7th U. S. Navy Symposium on Aeroballistics*, U. S. Naval Missile Center, Pt. Mugu, Calif., June 1966.

[6] Cooper, W. R., "Side Forces Resulting from Forward-Facing Steps and Injection Through a Slot in a Supersonic Flow," Mechanical Engineer's Thesis, California Institute of Technology, May 1965, Pasadena, Calif.

Decomposition of Second-Order Systems

S. KAUFMAN*

Bellcomm Inc., Washington, D. C.

IN areas such as structural feedback, flutter, and control systems in general, it is often convenient to formulate the problem as a set of linear second-order coupled equations. If the space is of order n these equations can be written as a set of $2n$ linear first-order coupled equations. This paper presents a method of finding the transformation to decouple the system. A situation where this decoupling cannot be fully carried out is also discussed.

Consider the following linear second-order matrix equation:

$$[A_1]\{\ddot{u}\} + [A_2]\{\dot{u}\} + [A_3]\{u\} = \{P(t)\} \tag{1}$$

where $[A_1]$, $[A_2]$, and $[A_3]$ are square matrices of order n containing constant coefficients (real or complex). These matrices are assumed to possess no preferred property such as symmetry or positive-definiteness.

Received December 12, 1969; revision received February 27, 1970.

* Member of the Technical Staff, Space Vehicle Dynamics Department, Structural Group. Associate Fellow AIAA.

Let

$$\{R\} = \begin{Bmatrix} \dot{u} \\ u \end{Bmatrix} \tag{2}$$

a partitioned vector of order $2n$ and recast Eq. (1) into the following format:

$$[B_1]\{\dot{R}\} + [B_2]\{R\} = \begin{Bmatrix} P(t) \\ 0 \end{Bmatrix} \tag{3}$$

where

$$[B_1] = \begin{bmatrix} A_1 & 0 \\ 0 & -I \end{bmatrix}$$

and

$$[B_2] = \begin{bmatrix} A_2 & A_3 \\ I & 0 \end{bmatrix}$$

Equation (3) can be partially hermitian symmetrized by premultiplying by $[B_1]^*$, the complex conjugate of $[B_1]$. The following expression is then obtained:

$$[H]\{\dot{R}\} + [B_1]^*[B_2]\{R\} = [B_{11}]^*\{P(t)\} \tag{4}$$

where $[H] = [B_1]^*[B_1]$, and $[B_{11}]^*$ is the matrix containing the first half of the columns of $[B_1]^*$. The hermitian matrix $[H]$ is non-negative-definite, and one can find its real eigenvalues $[d_1]$ and vectors $[\mathbf{v}]$ such that

$$[\mathbf{v}]^*[H][\mathbf{v}] = [d_1] = \begin{bmatrix} d & 0 \\ 0 & 0 \end{bmatrix}\begin{matrix}(p)\\(q)\end{matrix} \tag{5}$$

$$[\mathbf{v}]^*[\mathbf{v}] = [I]$$

and

$$p + q = 2n$$

The zero roots of $[H]$, if present, are those of $[A_1]$. After substituting

$$\{R\} = [\mathbf{v}]\begin{bmatrix} d^{-1} & 0 \\ 0 & I \end{bmatrix}\begin{matrix}\{s_1\}(p)\\\{s_2\}(q)\end{matrix} \tag{6}$$

into Eq. (4) and premultiplying by $[\mathbf{v}]^*$, one obtains the following expression:

$$\begin{bmatrix} I & 0 \\ 0 & 0 \end{bmatrix}\begin{Bmatrix} \dot{s}_1 \\ \dot{s}_2 \end{Bmatrix} + [D]\begin{Bmatrix} s_1 \\ s_2 \end{Bmatrix} = \begin{bmatrix} \beta \\ \alpha \end{bmatrix}\{P(t)\} \tag{7}$$

where

$$\begin{bmatrix} \beta \\ \alpha \end{bmatrix} = [\mathbf{v}^*][B_{11}]^*$$

and

$$[D] = \begin{bmatrix} D_{11} & D_{12} \\ D_{21} & D_{22} \end{bmatrix} = [\mathbf{v}]^*[B_1]^*[B_2][\mathbf{v}]\begin{bmatrix} d^{-1} & 0 \\ 0 & I \end{bmatrix}$$

From the bottom half of Eq. (7) one obtains the following:

$$\{s_2\} = -[D_{22}]^{-1}[D_{21}]\{s_1\} + [D_{22}]^{-1}[\alpha]\{P(t)\} \tag{8}$$

This solution is equivalent to the following:

$$\begin{Bmatrix} s_1 \\ s_2 \end{Bmatrix} = [F]\{s_1\} + \begin{bmatrix} 0 \\ D_{22}{}^{-1}\alpha \end{bmatrix}\{P(t)\} \tag{8a}$$

where

$$[F] = \begin{bmatrix} I \\ -D_{22}{}^{-1}D_{21} \end{bmatrix}$$

The following expression is obtained by substituting Eq. (8a) into Eq. (7) and premultiplying by $[F]^*$:

$$\{\dot{s}_1\} + [L]\{s_1\} = [\gamma]\{P(t)\} \tag{9}$$

where

$$[\gamma] = [\beta] - [D_{12}][D_{22}]^{-1}[\alpha]$$